

constraints. In the coldspot model, high-standing topography could also be created by convective shear tractions on the base of the lithosphere, leading to imbrication—the stacking of lithospheric thrust sheets. This process requires that new lithospheric surface area be created somewhere on Venus (e.g., lithospheric spreading); so far, this has not been observed. Addition of mass is usually required for compressional strain, and the hotspot model is actually attractive because new mass is provided vertically from the mantle by partial melting, and it is not necessary to obtain it horizontally from the lithosphere. Major strain associated with crustal plateaus might arise from crustal thickness instabilities [6,7] and from detachment [8] arising from eclogite formation in plateau roots.

Coronae: Coronae are large circular surface structures, which are observed in Magellan images to range up to 2600 km in diameter [9]; they are associated with both volcanism and tectonism. While it is generally agreed that coronae form in response to buoyantly rising material [9,10], there is no convergence of opinion on the nature of the diapir. Three endmember models are (1) thermal plumes from the mantle (which may then undergo pressure release partial melting), (2) compositional plumes that arise perhaps from melting induced by broader-scale thermal plumes, and (3) instabilities arising in regions that are partially molten or at the solidus [11,12]. In the last mechanism, the instability is triggered by an upward velocity perturbation, and on Venus such perturbations could arise from extensional strain events in the lithosphere associated with both upwelling and downwelling mantle flow. The coincidence of coronae with extensional features [9] provides evidence for this process.

Trenches and Subduction: On the basis of Venera 15–16 data, it has been proposed [13] that lithospheric convergence and underthrusting has occurred on the northern boundary of Ishtar Terra. The steep front and trench on the western side of Maxwell Montes also supports this idea. More recently, it has been suggested that trenches associated with the boundaries of certain large coronae mark the sites of “rollback” or retrograde subduction [14; see also 15]. In this hypothesis, the lithosphere associated with a corona extends outward and material is replaced by upward mantle flow (in analogy to terrestrial back-arc spreading). The expanding corona “consumes” lithosphere on its boundary (i.e., the surrounding lithosphere is subducted beneath the corona). The hypothesis for retrograde subduction is based on topographic and flexural analogy to terrestrial subduction trenches [14,15,16]. While evidence for outward migration of coronae is seen in the radar images, continuity of structures across proposed plate boundaries (i.e., trenches) argues against the subduction hypothesis [17].

Lithospheric subduction on Venus would require an active driving mechanism. No indication of spreading ridges is observed in the Magellan data, so “ridge push” can probably be discounted. Direct convective coupling from the underlying mantle may provide sufficient force, however [1]. The proposed retrograde subduction requires the lithosphere to be negatively buoyant. This may only be possible if garnet granulite or eclogite can form in the lower crust. The notion that the temperature gradient on Venus may be as low as $10^{\circ}/\text{km}$ (or less) in places [16] has implications for a relatively thick crust [18,19,20] and for the existence of such high-density phases encountered at depth in the lower crust before solidus temperatures are reached. However, the proposal that coronae mark the sites of mantle upwelling argues against such a low temperature gradient.

References: [1] Phillips R. J. et al. (1991) *Science*, 252, 288. [2] Bindschadler D. L. et al. (1992) *JGR*, special Magellan issue, in press. [3] Grimm R. E. et al. (1992) *LPSC XXIII*, 453–454.

- [4] Solomon S. C. et al. (1992) *JGR*, special Magellan issue, in press.
- [5] Kohlstedt D. L. (1992) In *Workshop on Mountain Belts on Venus and Earth*, 24, LPI, Houston.
- [6] Busse F. H. (1978) *Geophys. J. R. Astr. Soc.*, 52, 1–12.
- [7] Lenardic A. et al. (1991) *GRL*, 18, 2209–2212.
- [8] Turcotte D. L. (1989) *JGR*, 94, 2779–2785.
- [9] Stofan E. R. et al. (1992) *JGR*, special Magellan issue, in press.
- [10] Stofan E. R. and Head J. W. (1990) *Icarus*, 83, 216–243.
- [11] Tackley P. J. and Stevenson D. J. (1991) *Proceedings of NATO Advanced Study Institute*, in press.
- [12] Tackley P. J. and Stevenson D. J. (1991) *Eos*, 72, 287.
- [13] Head J. W. (1990) *Geology*, 18, 99–102.
- [14] Sandwell D. T. and Schubert G. (1992) *Science*, submitted.
- [15] McKenzie D. et al. (1992) *JGR*, special Magellan issue, in press.
- [16] Sandwell D. T. and Schubert G. (1992) *JGR*, special Magellan issue, in press.
- [17] Hansen V. L. et al., this volume.
- [18] Zuber M. T. (1987) *Proc. LPSC 17th*, in *JGR*, 92, E541–E551.
- [19] Grimm R. E. and Solomon S. C. (1988) *JGR*, 93, 11911–11929.
- [20] Zuber M. T. and Parmentier E. M. (1990) *Icarus*, 85, 290–308.

N93-14362

“PROBLEM” FOOTPRINTS IN MAGELLAN ALTIMETRY DATA. Jeffrey J. Plaut, Jet Propulsion Laboratory, MS 230–225, 4800 Oak Grove Drive, Pasadena CA 91109, USA.

Introduction: The intensity, time-delay, and frequency content of radar echoes from the Magellan altimetry system are reduced to several parameters that are of great use in addressing many geological issues of the surface of Venus. These parameters include planetary radius, power reflection coefficient (reflectivity, both uncorrected and corrected for diffuse scattering), rms slope, and scattering functions (the behavior of backscatter as a function of incidence angle) [1,2]. Because the surface of Venus often reflects radio energy in unpredictable ways, models of radar scattering and their associated algorithms occasionally fail to accurately solve for the above surface parameters. This paper presents methods for identifying possible “problem” altimetry data footprints, and techniques for resolving some key ambiguities.

Data Acquisition and Reduction: For each footprint, Magellan’s nadir-pointing altimeter transmits $1.1\text{-}\mu\text{s}$ bursts containing 17 pulses coded with a “chip” duration of $0.442\text{ }\mu\text{s}$. These constraints, combined with the delay response and the highly elliptical orbit, yield an effective along-track resolution of 8 to 20 km, and a cross-track resolution of 13 to 31 km [1]. The finest resolution is obtained near the periapsis latitude of 10°N , and the coarsest resolution is obtained at high latitudes. Processing in the frequency domain ensures that the along-track footprint dimension accurately reflects the sources of echo power. In the cross-track dimension, however, strong reflections from outside the footprint can contribute to the echo, leading to ambiguities in reduction to surface parameters [P. Ford, personal communication].

The primary standard data product generated from altimetry data is the Altimetry and Radiometry Composite Data Record (ARCDR) [3]. For each Magellan orbit, a separate file is produced for altimetry and radiometry data. For each footprint within the altimetry files, echo profiles, in range-sharpened and range-unsharpened formats, are included, along with the derived parameters such as radius, rms slope, and reflectivity, and best-fitting model echo “templates” from which the surface parameters are estimated. The radius estimate is from the template fit to the range-sharpened profile, while the rms slope and reflectivity estimates are from the template fit to the range-unsharpened profile. Examination of the echo profiles, and comparison to the templates selected to match the

profiles, provide useful information for resolving issues associated with "problem" footprints.

Case Studies: Sapas Mons. At a regional level, Magellan altimetry and SAR image data provide a consistent picture of Sapas Mons: a 400-km-diameter shield volcano that rises approximately 1.5 km above the surrounding elevated plain in western Atla Regio, to a maximum elevation of 6055.7 km radius. In the summit region, however, an apparent discrepancy is encountered between the morphology of structures seen in the SAR images and the radius measurements derived from the altimetry data. In particular, altimetry orbit 1467 passes directly across two scalloped dome structures at the volcano summit. While the SAR data clearly suggest these are positive in relief, eight altimetry footprints in orbit 1467 (11–13 and 16–20) have ARCDR radius values far below the typical summit region values of ~6055 km. Footprints 11–13, for example, have radius values more than 2 km below the preceding and following footprints (10 and 14, respectively). The combination of large fluctuations in radius values and apparent discrepancies between SAR and altimetry morphology provides an obvious "flag" that the derived altimetry data may contain spurious values.

Examination of the range-sharpened profiles and best-fit templates for the questionable footprints helps illuminate the possible source of the discrepancies. Figure 1 shows the profile and template used to determine the radius for footprint 20 of orbit 1467. The template echo, shown in a dashed line, is associated with a peak in the echo that appears to follow by 43 bins the leading edge of the measured echo. This delay of 43 0.21-μs bins corresponds to a round-trip travel time of 9.03 μs, giving an elevation difference of 1.35 km. Correcting the radius value of footprint 20 by this amount results in a value of 6055.2 km, consistent with surrounding footprints. Why should this echo contain two strong peaks, one of which produces a spuriously low radius value? Footprint 20 lies along the southwest flank of the southern summit dome feature. This suggests that echoes from the top of the dome may have "leaked" into the footprint, giving a spurious value for the area actually under consideration. For a given spacecraft altitude and time delay of a suspect echo peak, a family of combinations of feature height and feature offset from nadir can be calculated to understand the source of a secondary peak. Figure 2 shows a plot of such a family of geometries that could explain the secondary peak in footprint 20.

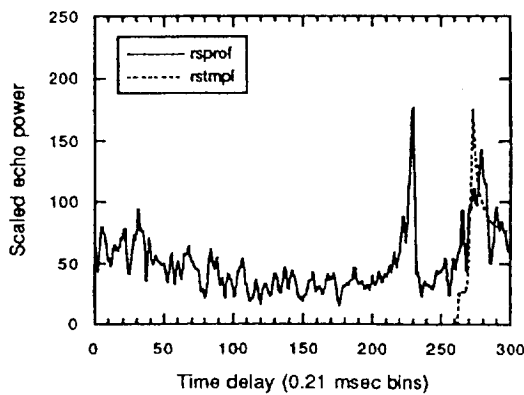


Fig. 1. Echo power vs. time delay, range-sharpened (rsprof), for orbit 1467, footprint 20 (Sapas Mons summit area). Also plotted is the best-fitting template from which the radius value was determined.

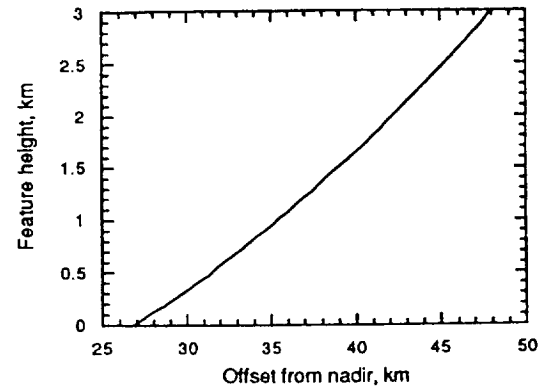


Fig. 2. Possible geometries to account for the secondary peak in the footprint 20 echo. A strong reflector at any combination of height and offset from nadir on the plotted curve will produce a secondary echo peak at the time delay seen in Fig. 1.

SAR data indicate that the dome sits within 25–30 km of the nadir, consistent with a dome height <0.5 km. The possibility that late echoes from outside the footprint can lead to spuriously low radius values increases toward periaxis, as the radius of curvature of the transmitted waveform becomes much smaller than that of the planet. This phenomenon may be responsible for the occasional topographic "holes" seen in low- to mid-latitude areas of rapidly varying relief.

Kuan Tao-sheng impact crater parabola. In the high southern latitudes southwest of Imdr Regio, several impact-related "parabola" features display highly anomalous scattering behavior [4]. Among these anomalous properties are unusually high values of rms slope and reflectivity in the ARCDR dataset. The two parameters are highly correlated along a narrow hairpin-shaped parabolic feature approximately 800 × 2000 km in size. Many of these surfaces show anomalously high cycle 1 SAR backscatter values when compared with cycle 2. Southeast of Kuan Tao-sheng Crater (45 km diameter), numerous altimetry footprints have "unphysical" ARCDR reflectivity values >1.0. The same footprints have ARCDR rms slope values in the range 8°–12°, unusually high for plains surfaces that appear relatively smooth in the SAR images, and relatively flat in radius (topography) data. The anomalous footprints frequently are surrounded by footprints with reasonable values, leading to sharp discontinuities. This combination of characteristics (unusually high rms slope and reflectivity values, apparent discrepancies with SAR and radius data, and sharp discontinuities), should again provide a "flag" that the altimetry data reduction procedure may have yielded spurious values. Examination of the range-unsharpened echo profiles and their associated templates indicates that while the leading edge of the echoes appears to have been accurately tracked, yielding accurate radius values, the wide dispersion of echo power with time may have led to spurious rms slope and reflectivity solutions. Apparently the statistics of height and slope distributions assumed in the Hagfors quasiprecular scattering model do not adequately describe the surface geometry within these footprints. The possible east-west asymmetry associated with these parabolic crater features [4] may account for the unusually wide dispersion of the echo. The analysis of scattering functions provided in the Surface Characteristics Vector Data Record (SCVDR) [2], in which fits to non-Hagfors scattering behavior are reported, will be of use in further

investigations of areas that display these unusual scattering characteristics.

References: [1] Pettengill G. H. et al. (1991) *Science*, 252, 260–265. [2] Tyler G. L. et al. (1992) *JGR*, special Magellan issue, in press. [3] Ford P. G. (1992) *ARCDR Software Interface Specification* (CD-ROM USA_NASA_JPL_MG_2001). [4] Plaut J. J. et al., this volume.

N93-14363

ANOMALOUS SCATTERING BEHAVIOR OF SELECTED IMPACT "PARABOLA" FEATURES: MAGELLAN CYCLE-TO-CYCLE COMPARISONS. J. J. Plaut¹, R. S. Saunders¹, E. R. Stofan¹, R. L. Kirk², G. G. Schaber², L. A. Soderblom², P. G. Ford³, G. H. Pettengill³, D. B. Campbell⁴, N. J. S. Stacy⁴, R. E. Arvidson⁵, and R. Greeley⁶. ¹Jet Propulsion Laboratory, MS 230-225, 4800 Oak Grove Drive, Pasadena CA 91109, USA, ²U. S. Geological Survey, Flagstaff AZ 86001, USA, ³Center for Space Research, Massachusetts Institute of Technology, Cambridge MA 02139, USA, ⁴National Astronomy and Ionospheric Center, Cornell University, Ithaca NY 14853, USA, ⁵Department of Earth and Planetary Sciences, Washington University, St. Louis MO 63130, USA, ⁶Department of Geology, Arizona State University, Tempe AZ 85287, USA.

Introduction: Magellan observations indicate that many venusian impact craters have associated surfaces, typically lower in backscatter and emissivity than the surroundings, that extend up to hundreds of kilometers to the west of craters, in parabolic planforms [1,2]. During Magellan's second mapping cycle, a number of these parabolic features were imaged for a second time, under a different viewing geometry. In some cases, the SAR backscatter appearance of portions of the parabolic features was quite different in the two datasets. In this paper, we present a description and preliminary interpretations of the anomalous appearance of these features as observed during Magellan's first and second mapping cycles.

Observations: Two types of structures within the parabolas show significant differences in appearance. These are "bright patches" and "streaks." Bright patches are irregular, diffuse-appearing areas of high backscatter (relative to surroundings). Values are typically 0 to 5 dB above the expected (Venus average) sigma zero, while surroundings are typically below the expected value. Differences in sigma zero between cycles can be as high as 9 dB, with comparable incidence angles but opposite look azimuths (cycle 1 east-looking, cycle 2 west-looking). Bright patches usually occur along the "arms" of the parabola features, but some are also seen in the central portions. Their distribution appears to be partly controlled by local small-scale (1–20 km) topography, such as wrinkle ridges. Discontinuous patches are often seen between (rather than straddling) wrinkle ridges, and some patches appear to terminate along ridges. Bright patch areas that are seen only in cycle 1 data occur at the craters Kuan Tao-sheng (−61.1, 181.7, 45 km), Eudocia (−59.1, 201.9, 29 km), and Boulanger (−26.5, 99.3, 57 km); patches seen only in cycle 2 data occur at the craters Stowe (−43.3, 233.2, 78 km), Kuan Tao-sheng, Austen (−25.0, 168.3, 47 km), Adaiah (−47.3, 253.3, 19 km), and Aksentyeva (−42.0, 271.9, 40 km).

"Streaks" are alternating high and low backscatter bands 1–20 km wide, up to 500 km long. The bright bands have still relatively low sigma zero values (within 2 dB of the expected), while the dark bands are almost always lower than the expected value. Streaks are often associated with, or are part of, bright patches. Trends of the streaks are consistently east-west, within about 10°. Like the bright

patches, streaks are commonly truncated along wrinkle ridges. Streaks are more common near the axes of the parabolas (i.e., due west of the crater), although some also are seen on the parabola arms. At Kuan Tao-sheng and Eudocia, streaks seen in cycle 1 SAR data are rarely seen in cycle 2. At Stowe, many streak sets are visible only in cycle 2 data, some are visible only in cycle 1 data, while others are visible in both datasets.

Several areas that show anomalous scattering behavior in cycle 1 and cycle 2 SAR data also have unusual properties in the cycle 1 radiometry and altimetry-derived datasets. In particular, the Eudocia/ Kuan Tao-sheng area, which shows an extensive (over 1500 × 2000 km) emissivity parabola, also displays extremely unusual behavior in the altimeter-derived reflectivity and rms slope parameters. The two parameters are highly correlated (high values in both) along a narrow hairpin-shaped parabolic feature approximately 800 × 2000 km in size. Many of the surfaces that show anomalously high cycle 1 SAR backscatter values (compared with cycle 2) occur on this hairpin-shaped feature. The magnitude of the rms slope (8°–10°) and reflectivity values (typically > 0.8; some >1.0) on otherwise smooth-appearing, moderately low emissivity plains, suggests that the altimeter echoes are not well-modeled by the Hagfors template matching procedure of [3]. Specifically, examination of the echo profiles shows that the anomalous areas have a wide dispersion in echo power with time. This accounts for the high rms slope solutions. The unphysical (>1.0) reflectivity values may result from a mismatch between the theoretical Hagfors quasispecular scattering formulation and the actual distribution of surface facets within the altimeter footprint.

To summarize the key observations: (1) The differences are only seen in association with impact crater parabola features. (2) The differences are seen in images taken with comparable incidence angles from opposite sides (at Kuan Tao-sheng/Eudocia, angles are within 5°, at Stowe within 3°). (3) The patterns of bright patched streaks are clearly associated with each other and with surface morphology (e.g., wrinkle ridges). (4) The most dramatic differences are confined to a single broad region of the planet: mid to high southern latitudes between Artemis and Phoebe. (5) The differences have both "senses," i.e., bright patches and streaks may be seen uniquely in either cycle 1 or cycle 2 data. (6) The Kuan Tao-sheng/ Eudocia area shows anomalously high reflectivity and rms slope values in altimetry-derived data.

Interpretations: The first issue that must be addressed is this: Are the apparent differences in SAR backscatter between cycle 1 and cycle 2 data a result of a modification of the surface (or subsurface) during the eight-month interval between data acquisitions, or are they a result of an azimuthally biased surface (or subsurface) structure in which backscatter is strongly enhanced in either the east- or west-looking configuration?

The best test of the surface change hypothesis involves duplicating the geometry of the cycle 1 acquisition. This experiment, in the Stowe Crater region, should have been conducted by the time of this colloquium, and relevant results will be presented. Cycle 1 and cycle 2 emissivity measurements, which were acquired at emission angles equivalent to the SAR incidence angles, show differences at the 2% level at Stowe and Kuan Tao-sheng, but the differences do not correlate well with the SAR differences. However, the bright patches and streaks do not have strong emissivity signatures in either cycle, so changes at the surface may not be detectable in emissivity. At present, altimetry-derived data from cycle 2 have not been reduced for these areas. The similar nadir-looking geometry of the cycle 1 and 2 altimetry measurements eliminates the look-